# The Kinetic of Atmospheric Acid Leaching of Brazilian Lateritic Nickel

**André L. A. Santos, Emily M. A. Becheleni, Rísia M. Papini, Paulo R. M. Viana and Sônia D. F. Rocha**

**Abstract** Atmospheric processing of nickel lateritic ores with low costs has been encouraged. In this work the kinetic of atmospheric acid leaching of a northern-Brazilian ore with 1.63% Ni and large amount of fine particles ($d_{50} \approx 0.075$ mm and 40% below 0.038 mm) is presented. Chemical analysis showed a trend of Ni and Fe concentration in finer fraction ($-0.075$ mm) and Si and Mg in the coarsest one ($-0.500 + 0.150$ mm) associated to distinct mineral phases. Nickel is widespread in the mineral matrix. Distinct behaviors were observed as a function of particle size associated to the distribution of silicates and iron oxides in the ore. The kinetic modeling indicated that leaching is controlled by porous layer diffusion at 65 °C, but at 95 °C exhibits a mixed control by porous layer diffusion in initial minutes (60 min) and by chemical reaction or diffusion through the pore layer in final minutes (60–240 min) depends on metal evaluated.

**Keywords** Nickel · Atmospheric leaching · Kinetic modeling
Mixed control · Lateritic ore

## Introduction

Nickel laterite ores represent, approximately, 60% of worlds nickel resources, but only 50% of the annual production of nickel comes from laterite sources [1]. Although the nickel can be found in sulfide deposits and processed by conventional methods of mineral processing, the laterite ore has become an additional source considering its increasing demand [2].

The evolution of laterite profile makes four different zones, which could contain nickel (ferricrete, limonites, transition and saprolite). It makes markedly variations into leaching behavior and the choice of processing route employed is driven by
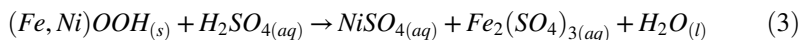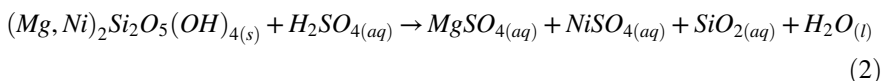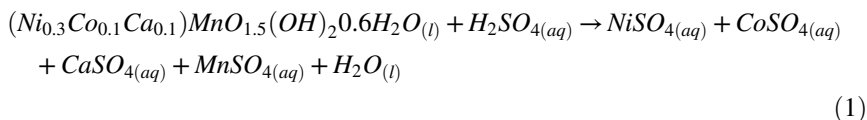
A. L. A. Santos · E. M. A. Becheleni · R. M. Papini · P. R. M. Viana · S. D. F. Rocha (✉)
Department of Mining Engineering, Federal University of Minas Gerais,
Av. Antônio Carlos, 6627, Bloco 2, Belo Horizonte 31270-901, Brazil
e-mail: sdrocha@demin.ufmg.br

technical, financial and environmental requirements [3]. In laterite ore nickel is finely disseminated into the iron oxides structures and magnesium silicates, instead of the presence of a specific nickel mineral [4–6]. This makes conventional mineral processing not applicable to increase the nickel grade into a concentrated fraction [7, 8]. Therefore, hydrometallurgical processing is the most indicated approach to this kind of ore because the mineral phases containing nickel need to be broken up to liberate the metal in leaching solution [9].

The study of atmospheric leaching has been encouraged instead of high-pressure acid leaching (HPAL) technology because it can be settled at low temperatures avoiding expensive HPAL autoclaves [10]. However, key issues related to kinetics parameters of nickel dissolution and subsequent steps of purification of liquor have to be addressed [11].

Recent studies about nickel leaching from laterite ores have revealed a strong dependence to mineralogy and chemistry association of nickel to mineral phases [12–14]. In this way, the source of laterite ore could influence on the leaching behavior.

The study of kinetics parameters of low-grade lateritic nickel ore is a challenge due to its complex mineralogy and the presence of many Ni and Co bearing minerals. The purposed mechanism of sulfuric atmospheric acid leaching may be splited in three equations: (1), (2) and (3) [15, 16]. These equations represent the proton attack to Ni/Co mineralized particles (asbolane, serpentines and goethite) and release of nickel and cobalt to a pregnant solution.

$$(Ni_{0.3}Co_{0.1}Ca_{0.1})MnO_{1.5}(OH)_2 0.6H_2O_{(l)} + H_2SO_{4(aq)} \rightarrow NiSO_{4(aq)} + CoSO_{4(aq)}$$
$$+ CaSO_{4(aq)} + MnSO_{4(aq)} + H_2O_{(l)}$$

$$(1)$$

$$(Mg, Ni)_2Si_2O_5(OH)_{4(s)} + H_2SO_{4(aq)} \rightarrow MgSO_{4(aq)} + NiSO_{4(aq)} + SiO_{2(aq)} + H_2O_{(l)}$$

$$(2)$$

$$(Fe, Ni)OOH_{(s)} + H_2SO_{4(aq)} \rightarrow NiSO_{4(aq)} + Fe_2(SO_4)_{3(aq)} + H_2O_{(l)} \qquad (3)$$

Although there are three main nickel-cobalt bearing minerals, overall, the controlling mechanism of leaching depends also on minor host minerals such as nontronite and magnetite [11]. Several kinetic models and reaction mechanism have been developed to identify the slowest step of leaching process [17]. In general, leaching of laterite ores follows shrinking core models which assumes the reaction wave develops progressively towards the center of particles through a porous layer in the particle.

Three steps, (i) proton diffusion through the liquid film and the porous layer, (ii) chemical reaction on the particle/porous surface and (iii) diffusion of reaction products through the porous layer and to the liquid film may control the reaction. The Eqs. (4), (5) and (6) represent the kinetics models of those controlling steps.

$$x = k_{VD} \cdot t \tag{4}$$

$$1 - 3(1-x)^{\frac{2}{3}} + 2(1-x) = k_{PL} \cdot t \tag{5}$$

$$1 - (1-x)^{\frac{1}{3}} = k_{CR} \cdot t \tag{6}$$

where $x$ is the fraction leached or dissolved metal, $k$ is the apparent rate constant and $t$ is time.

Equation 4 assumes that the controlling step is the volume diffusion (VD), Eq. 5 assumes control is due to diffusion in ash porous layer (PL) and Eq. 6 undertakes chemical reaction (CR) as the slowest step of process and controls the leaching.

Determination of activation energy $(E_a)$ for the reaction through Arrhenius correlation between apparent rate constant and absolute temperature (T) as show in the Eq. 7 helps in identifying the controlling step. In this equation R is the ideal gas constant and $k_0$ is the pre-exponential factor. $E_a$ is generally low for diffusion-controlled process ($<20$ kJ mol$^{-1}$) while to chemical reaction control the activation energy is higher ($>40$ kJ mol$^{-1}$)

$$k = k_0 \cdot e^{-\frac{E_a}{RT}} \tag{7}$$

Many authors have been studying the kinetics and the parameters associated to the dissolution time of nickel from laterite ores [4, 12, 13, 18–21]. However, the determination of reaction order with respect to nickel can be quite complex since there are multiples sources of nickel in the ore, as pointed out by [15, 16].

Kinetics studies of nickel leaching from laterite ores revealed a strong dependence on temperature which is mainly associated to chemical reaction control [4, 12, 13, 18]. However, other studies found a process control by diffusion into porous layer [18]. These authors found diffusion through porous layer was the controlling step to nickel extraction in any conditions of particle size and solid pulp densities. Nevertheless, cobalt diffusion into porous layer controlled the process at lower temperature (25 °C), but chemical reaction was determinant at higher temperature (90 °C). This inversion in the controlling steps suggests that a mixed process occurs, changing as function of temperature.

Control by mass transfer (diffusion) at lower temperature for chemical reaction is reported in literature [13, 22]. There is a correlation of temperature with the kinetics equation (Arrhenius equation) and in the diffusion coefficient [23]. These equations show different relation to temperature. While the Arrhenius equation depends on inverse exponential temperature, the diffusion coefficient is linearly dependent on temperature, which implies in more significant terms at higher temperatures for chemical reaction control.

Evaluation of the controlling steps of Ni leaching applying the Eqs. 4, 5 and 6 was carried out by MacCarthy et al. [12]. They indicated that only one controlling step was not enough to explain the kinetics observed. They divided the leaching time into two parts: one comprising the initial 30 min of reaction and the second

one the last 210 min. They found 40% of nickel extraction in the first minutes, level that reached 80% at the end of leaching time for particle size of −0.200 mm, 95 °C and pH 1.

The kinetics model split in two parts (until 30 min and from 30 to 240 min) shown better adjustment to the data. This division was applied, according to the authors, because there is mineral phases such as smectite (Mg-silicates) of easier dissolution, which occurs in the first minutes while the nickel associated to refractories minerals needs more time to be released from their structure [4, 12]. Although the study of kinetics was separated in two distinct period of time, the chemical reaction control was found for both.

Applying a detailed evaluation for Chinese lateritic ore, the authors concluded that the shrinking core model fitted the results, but in different moments there is a distinct step that controls the reaction [13]. In the first minutes, which are different for distinct temperatures analyzed, the control is chemical while the diffusion control was observed after 50 min of leaching. According to the authors, better kinetics parameter was found at 270 °C at which the resistance to diffusion is low.

In this paper the kinetics and the controlling steps of process for a Brazilian nickel laterite ore is evaluated. The sample was also characterized in order to identify the mineral phases and nickel bearing minerals, and the controlling step of leaching was evaluated through classical shrinking core model.

## Materials and Methods

### Sample and Characterizing

Laterite ore from Brazil was received in sets of 5 kg from the mining. It was sieved and dried at 60 °C for 24 h. After homogenization and sampling, samples were kept to physical, chemical and mineralogical characterization. Particle size distribution, X-ray diffractometer (XRD), scanning electron microscopy with chemical analysis (SEM/EDS) and atomic adsorption spectrometry (AAS) were applied to identify and quantify mineralogical phases and their association to nickel or to the particle size fractions. Fe, Mg, Mn and Co was also analysed besides nickel. After ore characterization fractions were prepared to leaching study.

### Leaching and Kinetic Evaluation

The experiments were carried out in a 1 L glass reactor equipped with Teflon impeller (400 rpm) and electrical heater, controlled by a thermostat (±0.1 °C). Leaching temperatures were set at 65 °C and 95 °C and ore fraction was added (−0.500 + 0.150 mm, −0.150 + 0.075 mm or −0.075 mm) to obtain a pulp

density of 20%. Experiments with 0.9 mol $L^{-1}$ sulfuric acid solution were developed to determine the mechanism control of leaching and the activation energy for Ni, Fe and Mg reactions. Samples were collected at 15, 30, 60, 120, 180, 240 min of leaching, vacuum filtered in filter paper with porosity of 8 μm, followed by filtration in fiberglass with porosity of 1 μm. Ni, Fe and Mg contents in liquor were quantified by atomic absorption spectrometry (AAS). Leaching control and the activation energy were evaluated trough the shrinking core model.
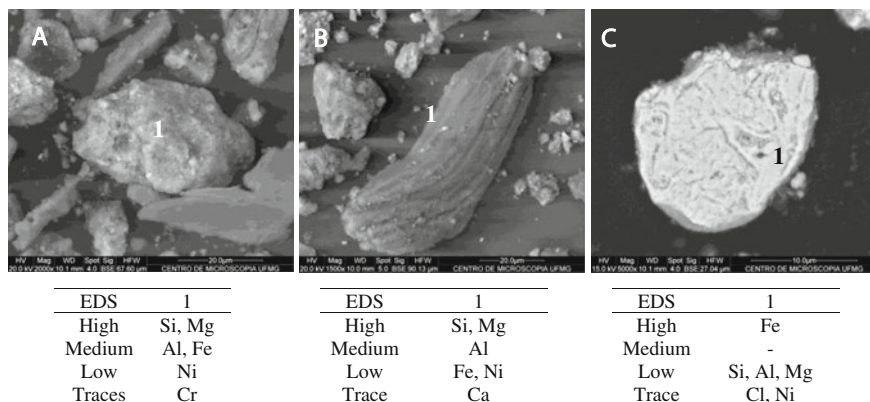
## Results and Discussion

### Sample Characterization

The particle size distribution of the ore shows that particles bellow 0.075 mm represent more than 50% of the ore and 44% of particles are smaller than 0.038 mm. Also, more than 20% are very tiny particles (below 0.010 mm), as expected for laterite ores, which contributes to suggest a transition to limonitic ore. These results are in good agreement with those reported by the literature [4, 5, 20, 24]. The characterization of particles including chemical and granulometry suggests a size-fractionating in −0.500 + 0.150 mm, −0.150 + 0.075 mm and −0.075 mm.

Quartz, chlorite, hematite, goethite and magnetite/maghemite were identified as major phases in this ore sample. This is also in a good agreement with nickel laterite ores from Indonesia, Iran, Australia, New Caledonia, China and Turkey [5, 25–28]. Some other mineral phases such as lizardite and chromite were detected too, but in small amounts.

Quantitative analysis, by Rietveld method, shows a concentration of Mg-minerals predominates in the coarser fraction (−0.500 + 0.150 mm) with 28% as lizardite and chlorite. The iron oxide phases, on the other hand, are concentrated in fine fraction (−0.075 mm) reaching up 56% with goethite being the main mineral corresponding to 42% of the fraction. In the full ore, Mg-minerals represent 25% with chlorite as major phase (21%), and iron oxide phases respond for 39% and being goethite 28% of sample. The −0.150 + 0.075 mm is a transitional fraction between −0.500 + 0.150 mm and −0.075 mm.

Ni is associated with oxides and silicates phases (Fig. 1) and as it was expected to this kind of ore, one specific mineral phase of nickel was not found, that was already indicated by the XRD analysis. The Ni contained in these deposits is mainly associated to specific mineral or it is closely associated to goethite by substitution of Fe in the crystalline structure [6, 29, 30], or it is incorporated into the magnesium silicates, explained by the aggressive weathering underwent by the rock [31].

According to quantitative chemical analysis presented in Table 1, Ni and Fe are concentrated in the ore fraction below 0.075 mm while Si shows another trend, being concentrated in the coarser fractions, above 0.075 mm. Additionally, the chemical analysis confirms iron oxide concentrates in the fine fraction and it is also

| EDS | 1 |
|-----|---|
| High | Si, Mg |
| Medium | Al, Fe |
| Low | Ni |
| Traces | Cr |

| EDS | 1 |
|-----|---|
| High | Si, Mg |
| Medium | Al |
| Low | Fe, Ni |
| Trace | Ca |

| EDS | 1 |
|-----|---|
| High | Fe |
| Medium | - |
| Low | Si, Al, Mg |
| Trace | Cl, Ni |

**Fig. 1** Back scattered electron images and energy dispersive X-ray spectroscopy analysis of Ni-bearing silicate (**a**) chlorite (**b**) and iron oxide (**c**)

**Table 1** Quantitative chemical analysis (%) of Brazilian laterite nickel ore

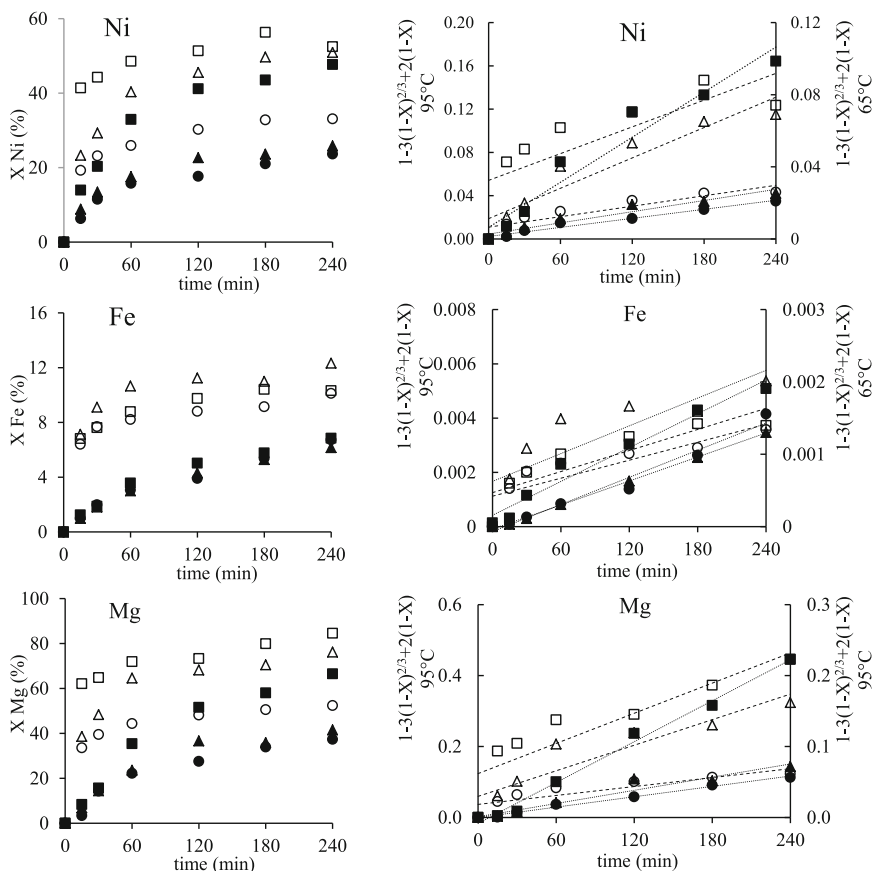| Particle size range | Ni | Fe | Si[a] | Mg | Co | Mn |
|---------------------|------|------|------|------|-------|-------|
| Global sample | 1.63 | 29.2 | 16.8 | 3.61 | 0.103 | 0.525 |
| −0.500 + 0.150 mm | 1.27 | 23.7 | 19.3 | 3.64 | 0.118 | 0.467 |
| −0.150 + 0.075 mm | 1,51 | 24,7 | 17.0 | 3.49 | 0,114 | 0.460 |
| −0.075 mm | 2.06 | 35.6 | 10.9 | 3.40 | 0.095 | 0.401 |

[a]Si was analyzed by ICP-OES

indicated that silicates are mostly in the coarser particles. Co and Mn do not show any accumulation profile in a specific range of particle size. Although Mg does not present concentration in any fraction, quantitative XRD analysis indicated that Mg-minerals (chlorite and lizardite) are concentrated in the coarser fraction.

Through this characterization and other summarized from the same ore, the total ore was fractionated in three samples with specific particle size range to evaluated the behavior in the leaching process and to access the kinetics study [32].

## Leaching Experiments and Leaching Process Step Control

Figure 2 presents nickel, iron and manganese extractions along leaching time. Elements extractions show different behaviors for distinct temperatures. Intermediate fraction (−0.150 + 0.075 mm) presents a transitional behavior since at lower temperature the extraction curve is like fraction −0.075 mm while at higher temperature it is similar to the coarser fraction (−0.500 + 0.150 mm). It can be clearly

**Fig. 2** Nickel, Iron and Magnesium extraction and its correspond correlation coefficient adjustment of the model best fit data, porous layer diffusion, for $-0.500 + 0.150$ mm, $-0150 + 0.075$ mm and $-0.075$ mm at 65 and 95 °C, solid-liquid ratio of 20%, initial sulphuric acid concentration 0.9 mol $L^{-1}$ and stirring rate of 400 rpm

observed that at 65 °C nickel extraction is similar for fractions $-0.150 + 0.075$ mm and $-0.075$ mm, however higher extractions were obtained for the coarser fraction.

Although nickel extractions were very distinct to each size fraction, concentrations in the liquor were approximately equal for all of them. It reaches 1525 mg $L^{-1}$ ($-0.500 + 0.15$ mm), 1023 mg $L^{-1}$ ($-0.150 + 0.075$ mm) and 1222 mg $L^{-1}$ ($-0.075$ mm) at 65 °C and 1672 mg $L^{-1}$ ($-0.500 + 0.15$ mm), 1923 mg $L^{-1}$ ($-0.150 + 0.075$ mm) and 1710 mg $L^{-1}$ ($-0.075$ mm) at 95 °C. This comes from

the difference between the Ni grades in distinct fractions and also due to mineralogy association of nickel and gangue minerals. Iron extraction average for three fractions raised from 6.5% (65 °C) to 11% (95 °C) being the concentration in the final liquor between 3811 and 6000 mg $L^{-1}$ (65 °C) and 5896 and 9000 mg $L^{-1}$ (95 °C). Therefore, extraction of Mg reached high level with concentrations of 6118 mg $L^{-1}$ and 7750 mg $L^{-1}$ (−0.500 + 0.150 mm at 65 and 95 °C). So, this behavior indicates that nickel in the fine fraction is major associated to iron oxide and in the coarser fraction with the silicates.

The kinetics analysis was completed applying the shrinking core model (Eqs. 4, 5 and 6) to three different size fractions and temperatures (Fig. 2 and Table 2).

At 95 °C, a single control for the whole period is not consistent with the data since there is a strong change in the slope of the linearized curve between 0 to 60 min and 60 to 240 min. It is verified that for 0 to 60 min process is controlled by diffusion into the porous layer, substantiated by the lower value of the kinetic constants and a better correlation coefficients ($R^2$) than obtained for volume diffusion and chemical reaction controlling mechanisms. From 60 to 240 min, the porous layer diffusion and chemical reaction models present similar adjustments ($R^2$) as well as the same order of apparent kinetic constants. Although some adjustments had low correlation coefficients (less than 0.90), the apparent velocity constants are lower in all fittings for the −0.075 mm fraction, corroborating that this

**Table 2** Apparent kinetic constant from better fit of shrinking core model and correlation coefficient ($R^2$) for leaching experiments at 95 °C, 0.9 mol $L^{-1}$ 20% solid-liquid ratio and 400 rpm

| Element | Fraction (mm) | Apparent kinetic constant (k–$min^{-1}$) for distinct models of control and correlation coefficient ($R^2$) | | | | | |
|---|---|---|---|---|---|---|---|
| | | Volume diffusion (♦) | | Porous layer (■) | | Chemical reaction (▲) | |
| | | 0–60 min | 60–240 min | 0–60 min | 60–240 min | 0–60 min | 60–240 min |
| Ni | −0.500 +0.150 | – | – | $1.5 \times 10^{-3}$ $R^2 = 0.7504$ | – | – | – |
| | −0.150 +0.075 | – | – | $1.1 \times 10^{-3}$ $R^2 = 0.9961$ | – | – | $3 \times 10^{-4}$ $R^2 = 0.9452$ |
| | −0.075 | – | – | $4 \times 10^{-4}$ $R^2 = 0.8596$ | $1 \times 10^{-4}$ $R^2 = 0.8927$ | – | – |
| Fe | −0.500 +0.150 | – | – | $4 \times 10^{-5}$ $R^2 = 0.8353$ | $6 \times 10^{-6}$ $R^2 = 0.8927$ | – | – |
| | −0.150 +0.075 | – | – | $6 \times 10^{-5}$ $R^2 = 0.9208$ | – | – | $3 \times 10^{-5}$ $R^2 = 0.7316$ |
| | −0.075 | – | – | $4 \times 10^{-5}$ $R^2 = 0.7829$ | – | – | $4 \times 10^{-5}$ $R^2 = 0.9607$ |
| Mg | −0.500 +0.150 | – | $7 \times 10^{-4}$ $R^2 = 0.9505$ | $4 \times 10^{-3}$ $R^2 = 0.7723$ | – | – | – |
| | −0.150 +0.075 | – | – | $3.4 \times 10^{-3}$ $R^2 = 0.9971$ | – | – | $5 \times 10^{-4}$ $R^2 = 0.9563$ |
| | −0.075 | – | – | $1.3 \times 10^{-3}$ $R^2 = 0.8647$ | $2 \times 10^{-4}$ $R^2 = 0.9836$ | – | – |

**Table 3** Apparent velocity constant and activation energy for the shrinking core model with porous layer diffusion control for experiments at initial acid concentration of 0.9 mol $L^{-1}$, 20% of solid-liquid ratio and stirring rate of 400 rpm 1 for the period between 0–60 min

| Element | Size fraction (mm) | Apparent velocity constant – k ($min^{-1}$) | | Activation energy ($kJ\ mol^{-1}$) |
|---|---|---|---|---|
| | | 65 °C | 95 °C | |
| Ni | −0.500 + 0.150 | $4 \times 10^{-4}$ | $1.4 \times 10^{-3}$ | 45.6 |
| | −0.150 + 0.075 | $1 \times 10^{-4}$ | $1.1 \times 10^{-3}$ | 82.8 |
| | −0.075 | $8 \times 10^{-4}$ | $4 \times 10^{-4}$ | 55.5 |
| Fe | −0.500 + 0.150 | $8 \times 10^{-6}$ | $4 \times 10^{-5}$ | 55.5 |
| | −0.150 + 0.075 | $6 \times 10^{-6}$ | $6 \times 10^{-5}$ | 79.5 |
| | −0.075 | $6 \times 10^{-6}$ | $4 \times 10^{-5}$ | 65.5 |
| Mg | −0.500 + 0.150 | $1 \times 10^{-3}$ | $4 \times 10^{-3}$ | 47.8 |
| | −0.150 + 0.075 | $3 \times 10^{-4}$ | $3.4 \times 10^{-3}$ | 83.8 |
| | −0.075 | $2 \times 10^{-4}$ | $1.3 \times 10^{-3}$ | 64.6 |

fraction limits the process. Table 3 shows the activation energies determined for Ni, Fe and Mg using the regression of the porous layer step as the process control for the period between 0–60 min.

The control by diffusion in porous layer was not expected, since several authors obtained the chemical reaction as a controlling step [4, 12, 13]. However, the widespread distribution of nickel in this ore may be the reason of this fact since nickel is disseminated into the mineral matrix and leaching greatly depend on reagents/products diffusion into the pores.

## Conclusions

Leaching of Brazilian nickel laterite ore under atmospheric acid leaching has shown a mixed control depending on temperature. The ore, mainly composed by Mg-silicates and Fe-oxides, contains Ni widespread into the mineral matrix, which affected the kinetic of leaching, in distinct way for different size fractions. In the fraction with sizes below 0.075 mm, 2.07% of Ni is associated to iron oxides while in the coarser fraction, Ni is associate to magnesium silicates. This difference in mineralogy associated to particle sizes affected the kinetic of leaching. For this particular ore, leaching is controlled by porous layer diffusion independently on particle size at 65 °C, however a mixed control is present at 95 °C. Therefore, activation energy is in order of chemical reaction mechanism for leaching process.

# References

1. USGS–United States Geological Survey (2018) Mineral Commodity Summaries 2018: U.S. Geological Survey. https://doi.org/10.3133/70194932. Accessed 22 Feb 2018
2. Norgate T, Jahanshahi S (2010) Low grade ores-smelt, leach or concentrate? Miner Eng 23(2):65–73. https://doi.org/10.1016/j.mineng.2009.10.002
3. Kyle J (2010) Nickel laterite processing technologies–where to next? Paper presented at ALTA 2010 Nickel/Cobalt/Copper Conference, Perth, Western Australia, 24–26 May 2010
4. MacCarthy J, Nosrati A, Skinner W, Addai-Mensah J (2016) Atmospheric acid leaching mechanisms and kinetics and rheological studies of low grade saprolitic nickel laterite ore. Hydrometallurgy 160:26–37. https://doi.org/10.1016/j.hydromet.2015.11.004
5. Panda L, Rao DS, Mishra BK, Das B (2014) Characterization and dissolution of low-grade ferruginous nickel lateritic ore by sulfuric acid. Miner Metal Process 31:57–65
6. Silva MLMC, Ramos AY, Tolentino HCN, Enzweiler J, Netto SM, Alves MCM (2003) Incorporation of Ni into natural goethite: an investigation by X-ray adsorption spectroscopy. Am Mineral 88:876–882. https://doi.org/10.2138/am-2003-5-617
7. Farrokhpay S, Filippov L (2016) Challenges in processing nickel laterite ores by flotation. Int J Miner Process 151:59–67. https://doi.org/10.1016/j.minpro.2016.04.007
8. Quast K, Connor JN, Skinner W, Robinson DJ, Addai-Mensah J (2015) Preconcentration strategies in the processing of nickel laterite ores Part 1: literature review. Miner Eng 79:261–268. https://doi.org/10.1016/j.mineng.2015.03.017
9. Dalvi AD, Bacon WG, Osborne RC (2004) The past and the future of nickel laterites. Paper presented at the PDCA 2004 international convention trade, trade show an investor exchange, Toronto, Ontário, 7–10 Mar 2004
10. Arroyo JC, Neudorf DA (2004) Atmospheric leach process for recovery of nickel and cobalt from limonite and saprolite ores. US Patent 6,680,035 B2. 20 Jan 2004
11. McDonald RG, Whittington BI (2008) Atmospheric acid leaching of nickel laterites review. Part I. sulphuric acid technologies. Hydrometallurgy 91:35–55. https://doi.org/10.1016/j.hydromet.2007.11.009
12. MacCarthy J, Nosrati A, Skinner W, Addai-Mensah J (2015) Acid leaching and rheological behaviour of siliceous goethitic nickel laterite ore: Influence of particle size and temperature. Miner Eng 77:52–63. https://doi.org/10.1016/j.mineng.2014.12.031
13. Liu K, Chen Q, Yin Z, Hu H, Ding Z (2012) Kinetics of leaching of Chinese laterite containing maghemite and magnetite in sulfuric acid solutions. Hydrometallurgy 125–126:125–136. https://doi.org/10.1016/j.hydromet.2012.06.001
14. Agatzini-Leonardu, S, Zafiratos IG (2004) Beneficiation of a Greek serpentinic nickeliferous ore: part II. Sulphuric acid heap and agitation leaching. Hydrometalurgy 74:267–275. https://doi.org/10.1016/j.hydromet.2004.05.006
15. Senanayake G, Childs J, Akerstron BD, Pugaev D (2011) Reductive acid leaching of laterite and metal oxides–a review with new data for Fe(Ni, Co)OOH and a limonitic ore. Hydrometallurgy 110:13–32. https://doi.org/10.1016/j.hydromet.2011.07.011
16. Rubisov DH, Krowinkel JM, Papangelakis VG (2000) Sulphuric acid pressure leaching of laterites–Universal kinetics of nickel dissolution for limonites and limonitic/saprolitic blends. Hydrometallurgy 58(1):1–11. https://doi.org/10.1016/s0304-386x(00)00094-3
17. Levenspiel O (1999) Chemical reaction engineering. Wiley, New York
18. Thubakgale CK, Mbaya RKK, Kabongo K (2013) A study of atmospheric acid leaching of a South African nickel laterite. Miner Eng 54:79–81. https://doi.org/10.1016/j.mineng.2013.04.006
19. Luo W, Feng Q, Ou L, Zhang G, Chen Y (2010) Kinetics of saprolitic laterite leaching by sulphuric acid at atmospheric pressure. Miner Eng 23(6):458–462. https://doi.org/10.1016/j.mineng.2009.10.006

20. Luo W, Feng Q, Ou L, Zhang G, Lu Y (2009) Fast dissolution of nickel from a lazardite-rich saprolitic by sulphuric acid at atmospheric pressure. Hydrometallurgy 96:171–175. https://doi.org/10.1016/j.hydromet.2008.08.001

21. Senanayake G, Das GK (2004) A comparative study of leaching kinetics of limonitic laterite and synthetic iron oxides in sulfuric acid containing sulphur dioxide. Hydrometallurgy 72:59–72. https://doi.org/10.1016/s0304-386x(03)00132-4

22. Amer AM, Ibrahim IA (2001) Aspects of leaching and kinetics of some Egyptian iron ore. Erzmetall J Explor Min Metall 54:619–624

23. Ghosh A, Ghosh S (2014) A textbook of metallurgical kinetics. PHI Learning Private Limited, Delhi

24. Fan R, Gerson AR (2013) Mineralogical characterisation of Indonesian laterites prior to and post atmospheric leaching. Hydrometallurgy 134–135:102–109. https://doi.org/10.1016/j.hydromet.2013.02.004

25. Mohammadreza F, Mohammad N, Ziaeddin SS (2014) Nickel extraction from low grade laterite by agitation leaching at atmospheric pressure. Int J Miner Sci Tech 24(4):543–548. https://doi.org/10.1016/j.ijmst.2014.05.019

26. Watling HR, Elliot AD, Fletcher HM, Robinson DJ, Sully DM (2011) Ore mineralogy of nickel laterites: controls on processing characteristics under simulated heap-leach conditions. Aust J Earth Sci 58:725–744. https://doi.org/10.1080/08120099.2011.602986

27. Liu K, Chen Q, Hu H, Yin Z (2010) Characterization and leaching behaviour of lizardite in Yuanjiang laterite ore. Appl Clay Sci 47(3–4):311–316. https://doi.org/10.1016/j.clay.2009.11.034

28. Andersen JCØ, Rollinson GK, Snook B, Herrington R, Fairhurst RJ (2009) Use of QEMSCAN® for the characterization of Ni-rich and Ni-poor goethite laterite ores. Miner Eng 22:1119–1129. https://doi.org/10.1016/j.mineng.2009.03.012

29. Puron AR (2001) Evidencias a favor de que la goethite es la principal portadora de niquel en los horizontes lateríticos de las cortezas ferroniqueliferas. Mineria y Geologia 18:21–31

30. Manceuau A, Schlegel ML, Musso M, Sole VA, Gauthier C, Petit PE, Trolard F (2000) Crystal chemistry of trace elements in natural and synthetic goethite. Geochimica et Cosmoquimica Acta, 64(21):3643–3661. https://doi.org/10.1016/s0016-7037(00)00427-0

31. Elias M (2002) Nickel laterite deposits–geological overview, resources and exploitation In: Cooke DR, Pongratz J (eds). Giant ore deposits: characteristics, genesis and exploitation. CODES Special Publication 4, Hobart, p 205–220

32. Santos ALA (2017) Caracterização e lixiviação atmosférica com ácido súlfurico de minério laterítico de níquel de deposito brasileiro. Master thesis, Universidade Federal de Minas Gerais